

Spatial Polarimetric Time-Frequency Distributions for Direction-of-Arrival Estimations

Yimin Zhang, *Senior Member, IEEE*, Baha Adnan Obeidat, *Student Member, IEEE*, and Moeness G. Amin, *Fellow, IEEE*

Abstract—Time-frequency distributions (TFDs) are traditionally applied to a single antenna receiver with a single polarization. Recently, spatial time-frequency distributions (STFDs) have been developed for receivers with multiple single-polarized antennas and successfully applied for direction-of-arrival (DOA) estimation of nonstationary signals. In this paper, we consider dual-polarized antenna arrays and extend the STFD to utilize the source polarization properties. The spatial polarimetric time-frequency distributions (SPTFDs) are introduced as a platform for processing polarized nonstationary signals, which are received by an array of dual-polarized double-feed antennas. This paper deals with narrow-band far-field point sources that lie in the plane of the receiver array. The source signals are decomposed into two orthogonal polarization components, such as vertical and horizontal. The ability to incorporate signal polarization empowers the STFDs with an additional degree of freedom, leading to improved signal and noise subspace estimates for direction finding. The polarimetric time-frequency MUSIC (PTF-MUSIC) method for DOA estimation based on the SPTFD platform is developed and shown to outperform the time-frequency, polarimetric, and conventional MUSIC techniques, when applied separately.

Index Terms—Array signal processing, direction-of-arrival (DOA) estimation, MUSIC, polarization, smart antennas, time-frequency distributions (TFDs).

I. INTRODUCTION

TIME-FREQUENCY distributions (TFDs) have been used for nonstationary signal analysis and synthesis in various areas, including speech, biomedicine, automotive industry, and machine monitoring [1], [2]. Over the past few years, the spatial dimension has been incorporated, along with the time and frequency variables, into quadratic and higher-order TFDs and led to the introduction of spatial time-frequency distributions (STFDs) for nonstationary array signal processing [3], [4]. The relationship between the TFDs of the sensor data and the TFDs of the individual source waveforms is defined by the steering, or the mixing, matrix, and was found to be similar to that encountered in the traditional covariance matrix approach to array

processing. This similarity has allowed subspace-based estimation methods to utilize the source instantaneous frequency for direction-finding. It has been shown that the MUSIC [5] and ESPRIT [6] techniques based on STFDs outperform their counterparts based on data covariance matrices, when applied for direction-of-arrival (DOA) estimation of sources of nonstationary temporal characteristics [4], [7]–[9].

Polarization and polarization diversities, on the other hand, are commonly used in wireless and satellite communications as well as various types of radar systems [10], [11]. Antenna and target polarization properties are widely employed in remote sensing and synthetic aperture radar (SAR) applications [12]–[14]. Airborne and spaceborne platforms as well as meteorological radars include polarization information [15], [16]. In addition, polarization plays an effective role for target identification in the presence of clutter [17], [18], and has also been incorporated in antenna arrays to improve signal parameter estimation, including DOA and time-of-arrival (TOA) [19]–[24].

The two important areas of time-frequency (t-f) signal representations and polarimetric signal processing have not been integrated or considered within the same platform, despite the extensive research work separately performed under each area. In this paper, we introduce the spatial polarimetric time-frequency distributions (SPTFDs) for double-feed dual-polarized arrays, where the source time-frequency and polarization signatures are concurrently utilized. The advantages of the proposed SPTFD platform are demonstrated using narrow-band farfield point-like emitters that lie in the plane of the receiver array. The signal polarization information empowers the STFDs with an additional degree of freedom, leading to improved spatial resolution and source discrimination.

The SPTFD is used to define the polarimetric time-frequency MUSIC (PTF-MUSIC) algorithm, which is formulated based on the source combined t-f and polarization properties and applied for DOA estimation of polarized nonstationary signals. The PTF-MUSIC technique is shown to outperform the MUSIC techniques that only incorporate either the t-f or the polarimetric source characteristics. The application to an ESPRIT-like method is introduced separately in [25].

This paper is organized as follows. Section II discusses the signal model and briefly reviews TFDs and STFDs. Section III considers dual-polarized antenna arrays and introduces the concept of SPTFDs. The PTF-MUSIC algorithm is proposed in Section IV. Sections V and VI, respectively, consider the issues of spatio-polarimetric correlations and DOA estimations of signals with time-varying polarization characteristics. Spatial and polarization averaging methods for coherent signal decorrelation

Manuscript received April 26, 2004; revised April 19, 2005. This work was supported in part by the ONR under Grant no. N00014-98-1-0176, DARPA under Grant no. MDA972-02-1-0022, and NSF under Grant EEC-0332490. The content of the information does not necessarily reflect the position or the policy of the Government, and no official endorsement should be inferred. The associate editor coordinating the review of this manuscript and approving it for publication was Dr. Ta-Hsin Li.

The authors are with the Center for Advanced Communications, Villanova University, Villanova, PA 19085 USA (e-mail: yimin@ieee.org; baha.obeidat@villanova.edu; moeness.amin@villanova.edu).

Digital Object Identifier 10.1109/TSP.2005.863124

are investigated in Section VII. Computer simulations, demonstrating the effectiveness of the proposed methods, are provided in Section VIII.

Throughout this paper, lower case bold and capital bold letters (e.g., \mathbf{a} and \mathbf{A}) are used to represent vectors and matrices, respectively. Moreover, $E[\cdot]$ denotes expectation operation, $(\cdot)^*$ denotes complex conjugate, $(\cdot)^T$ denotes transpose, and $(\cdot)^H$ denotes conjugate transpose (Hermitian). We use $(\cdot)^{[i]}$ to denote polarization i , $(\cdot)^{(k)}$ to denote the k th subarray. In addition, $\|\cdot\|$ denotes the vector norm, \otimes denotes Kronecker product operator, and \odot denotes Hadamard product operator.

II. SIGNAL MODEL

A. Time-Frequency Distributions

The Cohen's class of TFDs of a signal $x(t)$ is defined as [1]

$$D_{xx}(t, f) = \iint \varphi(t-u, \tau) x\left(u + \frac{\tau}{2}\right) \times x^*\left(u - \frac{\tau}{2}\right) e^{-j2\pi f\tau} dud\tau \quad (1)$$

where t and f represent the time and frequency indexes, respectively and $j = \sqrt{-1}$. The kernel $\varphi(t, \tau)$ uniquely defines the TFD and is a function of the time and lag variables. In this paper, all the integrals are from $-\infty$ to ∞ .

The cross-term TFD of two signals $x_k(t)$ and $x_l(t)$ is defined by

$$D_{x_k x_l}(t, f) = \iint \varphi(t-u, \tau) x_k\left(u + \frac{\tau}{2}\right) \times x_l^*\left(u - \frac{\tau}{2}\right) e^{-j2\pi f\tau} dud\tau. \quad (2)$$

B. Spatial Time-Frequency Distributions

The STFDs have already been developed for single-polarized antenna arrays [4], [7]. Consider a narrow-band direction-finding problem where the signal bandwidth is small relative to its carrier frequency. We note that the wide-band array processing for nonstationary signals, which has been examined in [26] and [27], is outside the scope of the proposed approach. The following linear data model is assumed:

$$\mathbf{x}(t) = \mathbf{y}(t) + \mathbf{n}(t) = \mathbf{A}\mathbf{s}(t) + \mathbf{n}(t) \quad (3)$$

where the $m \times n$ matrix $\mathbf{A} = [\mathbf{a}_1, \mathbf{a}_2, \dots, \mathbf{a}_n]$ is the mixing matrix that holds the spatial information. The number of array elements is m , whereas n represents the number of signals incident on the array. In the above equation, $\mathbf{A} = \mathbf{A}(\Phi) = [\mathbf{a}(\phi_1), \mathbf{a}(\phi_2), \dots, \mathbf{a}(\phi_n)]$, where $\Phi = [\phi_1, \phi_2, \dots, \phi_n]$ and $\mathbf{a}(\phi_k)$ is the spatial signature for source k . Each element of the $n \times 1$ vector $\mathbf{s}(t) = [s_1(t) \ s_2(t) \ \dots \ s_n(t)]^T$ is a monocomponent signal. Due to the mixing at each sensor, the elements of the $m \times 1$ sensor data vector $\mathbf{x}(t)$ become multicomponent signals. $\mathbf{n}(t)$ is an $m \times 1$ additive noise vector, which consists of independent zero-mean, white, and Gaussian distributed processes.

The STFD of a data vector $\mathbf{x}(t)$ is expressed as [3]

$$\mathbf{D}_{\mathbf{xx}}(t, f) = \iint \varphi(t-u, \tau) \mathbf{x}\left(u + \frac{\tau}{2}\right) \times \mathbf{x}^H\left(u - \frac{\tau}{2}\right) e^{-j2\pi f\tau} dud\tau \quad (4)$$

where the (k, l) th element of $\mathbf{D}_{\mathbf{xx}}(t, f)$ is given by (2) for $k, l = 1, 2, \dots, m$. The noise-free STFD is obtained by substituting (3) in (4)

$$\mathbf{D}_{\mathbf{xx}}(t, f) = \mathbf{A}(\Phi) \mathbf{D}_{\mathbf{ss}}(t, f) \mathbf{A}^H(\Phi) \quad (5)$$

where $\mathbf{D}_{\mathbf{ss}}(t, f)$ is the TFD matrix of $\mathbf{s}(t)$ which consists of auto- and cross-source TFDs. With the presence of the noise, which is uncorrelated with the signals, the expected value $\mathbf{D}_{\mathbf{xx}}(t, f)$ yields

$$E[\mathbf{D}_{\mathbf{xx}}(t, f)] = \mathbf{A}(\Phi) E[\mathbf{D}_{\mathbf{ss}}(t, f)] \mathbf{A}^H(\Phi) + \sigma^2 \mathbf{I}. \quad (6)$$

In the above equation, σ^2 is the noise power, \mathbf{I} is the identity matrix, and $E[\cdot]$ denotes the statistical expectation operator.

Equation (6) is similar to the commonly used formula in narrow-band array processing problems, relating the source covariance matrix to the sensor spatial covariance matrix. Here, the covariance matrices are replaced by the source and sensor TFD matrices. The two subspaces spanned by the principle eigenvectors of $\mathbf{D}_{\mathbf{xx}}(t, f)$ and the columns of $\mathbf{A}(\Phi)$ are, therefore, identical. The STFD matrix can be constructed from the t-f points with highly localized signal energy, thus allowing the corresponding signal and noise subspace estimates to be more robust to noise than their counterparts obtained using the data covariance matrix, $\mathbf{R}_{\mathbf{xx}} = E[\mathbf{x}(t)\mathbf{x}^H(t)]$ [4], [8], [9]. Further, the source discriminations, provided through the flexibility of selecting t-f points or regions, permit DOA estimations to be performed for only individual or subgroup of sources. In this respect, the number of impinging sources can exceed the number of array sensors. The above attractive properties allow key problems in various array processing applications to be addressed and solved using a new formulation (6), which is more tuned to nonstationary signal environments.

III. SPATIAL POLARIMETRIC TIME-FREQUENCY DISTRIBUTIONS

A. Polarimetric Modeling

For a transverse electromagnetic (TEM) wave incident on the array, shown in Fig. 1, the electric field can be described as

$$\begin{aligned} \vec{E}(t) &= E_\theta(t)\hat{\theta} + E_\phi(t)\hat{\phi} \\ &= [E_\theta(t)\cos(\theta)\cos(\phi) - E_\phi(t)\sin(\phi)]\hat{x} \\ &\quad + [E_\theta(t)\cos(\theta)\sin(\phi) + E_\phi(t)\cos(\phi)]\hat{y} \\ &\quad + E_\theta(t)\sin(\theta)\hat{z} \end{aligned} \quad (7)$$

where $\hat{\phi}$ and $\hat{\theta}$ are, respectively, the spherical unit vectors along the azimuth and elevation angles ϕ and θ , viewed from the source. The unit vectors \hat{x} , \hat{y} and \hat{z} are defined along the x , y , and z directions, respectively. For simplicity and without loss of generality, it is assumed that the source signal is in the

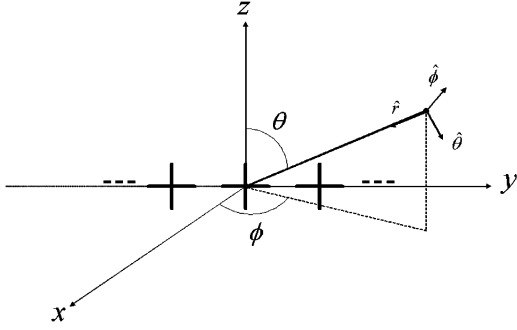


Fig. 1. Dual-polarized array.

$x - y$ plane, whereas the array is located in the $y - z$ plane. Accordingly, $\theta = 90^\circ$, $\hat{\theta} = -\hat{z}$, and

$$\vec{E}(t) = -E_\phi(t) \sin(\phi) \hat{x} + E_\phi(t) \cos(\phi) \hat{y} + E_\theta(t) \hat{z}. \quad (8)$$

We denote $s(t)$ as the source magnitude measured at the receiver reference sensor, with polarization angle $\gamma \in [0, \pi/2]$, and polarization phase difference $\eta \in (-\pi, \pi]$. The source horizontal and vertical polarization components, $s^{[v]}(t)$ and $s^{[h]}(t)$, can then be expressed in terms of the respective spherical fields, $E_\theta(t)$ and $E_\phi(t)$, as

$$E_\theta(t) = s^{[v]}(t) = s(t) \cos(\gamma), \quad (9)$$

$$E_\phi(t) = s^{[h]}(t) = s(t) \sin(\gamma) e^{j\eta}. \quad (10)$$

A signal is referred to as linearly polarized if $\eta = 0$ or $\eta = 180$ degrees. Substituting (9) and (10) in (8) results in

$$\vec{E}(t) = s(t) [-\cos(\gamma) \sin(\phi) \hat{x} + \cos(\phi) \sin(\gamma) e^{j\eta} \hat{y} + \cos(\gamma) \hat{z}]. \quad (11)$$

Now we consider that n signals impinge on the array, consisting of m dual-polarized antennas. The vertical and horizontal components of the k th source are expressed as

$$\begin{aligned} s_k^{[v]}(t) &= s_k(t) \cos(\gamma_k) \triangleq c_{k1} s_k(t) \\ s_k^{[h]}(t) &= s_k(t) \sin(\gamma_k) e^{j\eta_k} \triangleq c_{k2} s_k(t) \end{aligned} \quad (12)$$

where the parameters $c_{k1} = \cos(\gamma_k)$ and $c_{k2} = \sin(\gamma_k) e^{j\eta_k}$ denote the vertical and horizontal polarization coefficients. The corresponding signal received at the l th dual-polarized antenna, with vertical and horizontal antennas located in the \hat{z} and \hat{y} directions, is expressed as

$$\begin{aligned} \underline{y}_l(t) &= [y_l^{[v]}(t), y_l^{[h]}(t)]^T = \sum_{k=1}^n [a_{kl}^{[v]} \vec{E}_k \cdot \hat{z}, a_{kl}^{[h]} \vec{E}_k \cdot \hat{y}]^T \\ &= \sum_{k=1}^n [a_{kl}^{[v]} s_k^{[v]}(t), a_{kl}^{[h]} s_k^{[h]}(t) \cos(\phi_k)]^T \end{aligned} \quad (13)$$

where “ \cdot ” represents the dot product, \vec{E}_k is the electric-field vector corresponding to the k th source, and $a_{kl}^{[v]}$ and $a_{kl}^{[h]}$, respectively, are the l th elements of the vertically and horizontally polarized array vectors, $\mathbf{a}^{[v]}(\phi_k)$ and $\mathbf{a}^{[h]}(\phi_k)$. It is assumed that the array has been calibrated and both $\mathbf{a}^{[v]}(\phi)$ and $\mathbf{a}^{[h]}(\phi)$ are known and normalized such that $\|\mathbf{a}^{[v]}(\phi)\|^2 = \|\mathbf{a}^{[h]}(\phi)\|^2 = m$. It is noted that the $\cos(\phi_k)$ term in the horizontally polarized array manifold can be absorbed in the array calibration over the

region of interest and, therefore, removed from further consideration. Then, the above equation is simplified as

$$\begin{aligned} \underline{y}_l(t) &= [a_{kl}^{[v]} s_k^{[v]}(t), a_{kl}^{[h]} s_k^{[h]}(t)]^T \\ &= s_k(t) \left([a_{kl}^{[v]} \ a_{kl}^{[h]}]^T \odot [c_{k1} \ c_{k2}]^T \right) \\ &\triangleq s_k(t) \mathbf{a}_{kl} \odot \mathbf{c}_k \end{aligned} \quad (14)$$

where the vector $\mathbf{c}_k = [c_{k1}, c_{k2}]^T = [\cos(\gamma_k), \sin(\gamma_k) e^{j\eta_k}]$ represents the polarization signature of the k th source.

B. Polarimetric Time-Frequency Distributions

For a dual-polarized sensor, k , we define the self- and cross-polarized TFDs, respectively, as

$$\begin{aligned} D_{x_k^{[i]} x_k^{[i]}}(t, f) &= \iint \varphi(t - u, \tau) x_k^{[i]} \left(u + \frac{\tau}{2} \right) \\ &\quad \times \left(x_k^{[i]} \left(u - \frac{\tau}{2} \right) \right)^* e^{-j2\pi f \tau} du d\tau \end{aligned} \quad (15)$$

and

$$\begin{aligned} D_{x_k^{[i]} x_k^{[j]}}(t, f) &= \iint \varphi(t - u, \tau) x_k^{[i]} \left(u + \frac{\tau}{2} \right) \\ &\quad \times \left(x_k^{[j]} \left(u - \frac{\tau}{2} \right) \right)^* e^{-j2\pi f \tau} du d\tau \end{aligned} \quad (16)$$

where the superscripts i and j denote either v or h . The self- and cross-polarized TFDs constitute the 2×2 polarimetric TFD (PTFD) matrix

$$\begin{aligned} \mathbf{D}_{\underline{x}_k \underline{x}_k}(t, f) &= \iint \varphi(t - u, \tau) \underline{x}_k \left(u + \frac{\tau}{2} \right) \underline{x}_k^H \left(u - \frac{\tau}{2} \right) \\ &\quad \times e^{-j2\pi f \tau} du d\tau. \end{aligned} \quad (17)$$

The diagonal entries of $\mathbf{D}_{\underline{x}_k \underline{x}_k}(t, f)$ are the self-polarized TFDs, $D_{x_k^{[i]} x_k^{[i]}}(t, f)$, whereas the off-diagonal elements are the cross-polarized terms $D_{x_k^{[i]} x_k^{[j]}}(t, f)$, $i \neq j$.

C. Spatial Polarimetric Time-Frequency Distributions

Equations (13)–(17) correspond to the case of a single dual-polarization sensor. With an m -sensor array, the data vector, for each polarization i , $i = v$ or h , is expressed as

$$\begin{aligned} \mathbf{x}^{[i]}(t) &= [x_1^{[i]}(t), x_2^{[i]}(t), \dots, x_m^{[i]}(t)]^T = \mathbf{y}^{[i]}(t) + \mathbf{n}^{[i]}(t) \\ &= \mathbf{A}^{[i]}(\Phi) \mathbf{s}^{[i]}(t) + \mathbf{n}^{[i]}(t). \end{aligned} \quad (18)$$

The generalization of single-sensor polarimetric time-frequency distributions to a multi-sensor receiver is obtained using (18). Instead of the scalar variable TFD of (15), we define the self-polarized STFD matrix of vector $\mathbf{x}^{[i]}(t)$ for polarization i as

$$\begin{aligned} \mathbf{D}_{\mathbf{x}^{[i]} \mathbf{x}^{[i]}}(t, f) &= \iint \varphi(t - u, \tau) \mathbf{x}^{[i]} \left(u + \frac{\tau}{2} \right) \\ &\quad \times \left(\mathbf{x}^{[i]} \left(u - \frac{\tau}{2} \right) \right)^H e^{-j2\pi f \tau} du d\tau, \end{aligned} \quad (19)$$

which, in the noise-free environment, can be expressed as

$$\mathbf{D}_{\mathbf{x}^{[i]} \mathbf{x}^{[i]}}(t, f) = \mathbf{A}^{[i]}(\Phi) \mathbf{D}_{\mathbf{s}^{[i]} \mathbf{s}^{[i]}}(t, f) \left(\mathbf{A}^{[i]}(\Phi) \right)^H. \quad (20)$$

In a similar manner, the cross-polarization STFD matrix between the data vectors with two different polarizations i and j can be expressed as

$$\mathbf{D}_{\mathbf{x}^{[i]}\mathbf{x}^{[j]}}(t, f) = \iint \varphi(t-u, \tau) \mathbf{x}^{[i]} \left(u + \frac{\tau}{2}\right) \times \left(\mathbf{x}^{[j]} \left(u - \frac{\tau}{2}\right)\right)^H e^{-j2\pi f\tau} du d\tau \quad (21)$$

which becomes

$$\mathbf{D}_{\mathbf{x}^{[i]}\mathbf{x}^{[j]}}(t, f) = \mathbf{A}^{[i]}(\Phi) \mathbf{D}_{\mathbf{s}^{[i]}\mathbf{s}^{[j]}}(t, f) \left(\mathbf{A}^{[j]}(\Phi)\right)^H \quad (22)$$

when the noise is ignored.

Based on (18), the following extended data vector can be constructed for both polarizations

$$\begin{aligned} \mathbf{x}(t) &= \begin{bmatrix} \mathbf{x}^{[v]}(t) \\ \mathbf{x}^{[h]}(t) \end{bmatrix} \\ &= \begin{bmatrix} \mathbf{A}^{[v]}(\Phi) & \mathbf{0} \\ \mathbf{0} & \mathbf{A}^{[h]}(\Phi) \end{bmatrix} \begin{bmatrix} \mathbf{s}^{[v]}(t) \\ \mathbf{s}^{[h]}(t) \end{bmatrix} + \begin{bmatrix} \mathbf{n}^{[v]}(t) \\ \mathbf{n}^{[h]}(t) \end{bmatrix} \\ &= \begin{bmatrix} \mathbf{A}^{[v]}(\Phi) & \mathbf{0} \\ \mathbf{0} & \mathbf{A}^{[h]}(\Phi) \end{bmatrix} \begin{bmatrix} \mathbf{Q}^{[v]} \\ \mathbf{Q}^{[h]} \end{bmatrix} \mathbf{s}(t) + \begin{bmatrix} \mathbf{n}^{[v]}(t) \\ \mathbf{n}^{[h]}(t) \end{bmatrix} \\ &= \mathbf{B}(\Phi) \mathbf{Q} \mathbf{s}(t) + \mathbf{n}(t), \end{aligned} \quad (23)$$

where

$$\mathbf{B}(\Phi) = \begin{bmatrix} \mathbf{A}^{[v]}(\Phi) & \mathbf{0} \\ \mathbf{0} & \mathbf{A}^{[h]}(\Phi) \end{bmatrix} \quad (24)$$

is block-diagonal, and

$$\mathbf{Q} = \begin{bmatrix} \mathbf{Q}^{[v]} \\ \mathbf{Q}^{[h]} \end{bmatrix} \quad (25)$$

is the polarization signature vector of the sources, where

$$\begin{aligned} \mathbf{q}^{[v]} &= [\cos(\gamma_1), \dots, \cos(\gamma_n)]^T \\ \mathbf{Q}^{[v]} &= \text{diag}(\mathbf{q}^{[v]}) \end{aligned} \quad (26)$$

$$\begin{aligned} \mathbf{q}^{[h]} &= [\sin(\gamma_1)e^{j\eta_1}, \dots, \sin(\gamma_n)e^{j\eta_n}]^T \\ \mathbf{Q}^{[h]} &= \text{diag}(\mathbf{q}^{[h]}). \end{aligned} \quad (27)$$

Accordingly

$$\begin{aligned} \mathbf{B}(\Phi) \mathbf{Q} &= \begin{bmatrix} \mathbf{a}^{[v]}(\phi_1) \cos(\gamma_1) & \dots & \mathbf{a}^{[v]}(\phi_n) \cos(\gamma_n) \\ \mathbf{a}^{[h]}(\phi_1) \sin(\gamma_1) e^{j\eta_1} & \dots & \mathbf{a}^{[h]}(\phi_n) \sin(\gamma_n) e^{j\eta_n} \end{bmatrix} \\ &= [\tilde{\mathbf{a}}(\phi_1) \ \dots \ \tilde{\mathbf{a}}(\phi_n)]. \end{aligned} \quad (28)$$

The above matrix can be viewed as the extended mixing matrix, with $\mathbf{a}(\phi_k)$ representing the joint spatial-polarimetric signature of signal k . The extended spatial polarization signature vector for the k th source is

$$\tilde{\mathbf{a}}(\phi_k) = \begin{bmatrix} \mathbf{a}^{[v]}(\phi_k) \cos(\gamma_k) \\ \mathbf{a}^{[h]}(\phi_k) \sin(\gamma_k) e^{j\eta_k} \end{bmatrix}. \quad (29)$$

It is clear that the dual-polarization array, compared to single-polarization case, doubles the vector space dimensionality.

It is now possible to combine the polarimetric, spatial, and t-f properties of the source signals incident on the receiver array. The STFD of the dual-polarization data vector $\mathbf{x}(t)$ can be written as

$$\mathbf{D}_{\mathbf{xx}}(t, f) = \iint \varphi(t-u, \tau) \mathbf{x} \left(u + \frac{\tau}{2}\right) \times \mathbf{x}^H \left(u - \frac{\tau}{2}\right) e^{-j2\pi f\tau} du d\tau. \quad (30)$$

$\mathbf{D}_{\mathbf{xx}}(t, f)$, formulated in (30), is referred to as the SPTFD matrix. This distribution, or matrix, serves as a general framework within which typical problems in array processing, including direction-finding, can be addressed, as shown in the next section.

When the effect of noise is ignored, the SPTFD matrix is related to the source TFD matrix by

$$\mathbf{D}_{\mathbf{xx}}(t, f) = \mathbf{B}(\Phi) \mathbf{Q} \mathbf{D}_{\mathbf{ss}}(t, f) \mathbf{Q}^H \mathbf{B}^H(\Phi). \quad (31)$$

IV. POLARIMETRIC TIME-FREQUENCY MUSIC

Time-frequency MUSIC (TF-MUSIC) has been recently introduced to improve spatial resolution of sources with clear t-f signatures [7]. The proposed PTF-MUSIC is an important generalization of the TF-MUSIC for dealing with polarized signals and polarized arrays. It is based on the search for the minimum values of the orthogonal projection of the array vector, defined in the joint spatial and polarimetric domains, on the noise subspace obtained from the SPTFD matrix over selected t-f regions.

Consider the following spatial signature matrix:

$$\mathbf{F}(\phi) = \frac{1}{\sqrt{m}} \begin{bmatrix} \mathbf{a}^{[v]}(\phi) & \mathbf{0} \\ \mathbf{0} & \mathbf{a}^{[h]}(\phi) \end{bmatrix} \quad (32)$$

corresponding to DOA ϕ . Since $\|\mathbf{a}^{[i]}(\phi)\|^2 = m$, $\mathbf{F}^H(\phi) \mathbf{F}(\phi)$ is the 2×2 identity matrix.

To search in the joint spatial and polarimetric domains, we define the following spatio-polarimetric search vector:

$$\mathbf{f}(\phi, \mathbf{c}) = \frac{\mathbf{F}(\phi) \mathbf{c}}{\|\mathbf{F}(\phi) \mathbf{c}\|} = \mathbf{F}(\phi) \mathbf{c} \quad (33)$$

where the vector $\mathbf{c} = [c_1 \ c_2]^T$ is a unit norm vector with unknown polarization coefficients. In (33), we have used the fact that $\|\mathbf{F}(\phi) \mathbf{c}\| = [\mathbf{c}^H \mathbf{F}^H(\phi) \mathbf{F}(\phi) \mathbf{c}]^{1/2} = (\mathbf{c}^H \mathbf{c})^{1/2} = 1$.

The PTF-MUSIC spectrum is given by the following function:

$$\begin{aligned} P(\phi) &= \left[\min_{\mathbf{c}} \mathbf{f}^H(\phi, \mathbf{c}) \mathbf{U}_n \mathbf{U}_n^H \mathbf{f}(\phi, \mathbf{c}) \right]^{-1} \\ &= \left[\min_{\mathbf{c}} \mathbf{c}^H \mathbf{F}^H(\phi) \mathbf{U}_n \mathbf{U}_n^H \mathbf{F}(\phi) \mathbf{c} \right]^{-1} \end{aligned} \quad (34)$$

where \mathbf{U}_n is the noise subspace obtained from the SPTFD matrix in (30) using selected t-f points. For t-f-based DOA estimation methods, t-f averaging and joint block-diagonalization are two known techniques that can be used to integrate the different STFD or SPTFD matrices constructed at multiple t-f points [4], [7], [30]. The selection of those points from high energy concentration regions pertaining to all or some of the sources enhances

the SNR and allows the t-f based MUSIC algorithms to be more robust to noise [4] compared to its conventional MUSIC counterpart.

In (34), the term in brackets is minimized by finding the minimum eigenvalue of the 2×2 matrix $\mathbf{F}^H(\phi)\mathbf{U}_n\mathbf{U}_n^H\mathbf{F}(\phi)$. Thus, a computationally expensive search in the polarization domain is avoided by performing a simple eigen-decomposition on a 2×2 matrix. As a result, the PTF-MUSIC spectrum can be expressed as

$$P(\phi) = \lambda_{\min}^{-1} [\mathbf{F}^H(\phi)\mathbf{U}_n\mathbf{U}_n^H\mathbf{F}(\phi)] \quad (35)$$

where $\lambda_{\min}[\cdot]$ denotes the minimum eigenvalue operator. The DOAs of the sources are estimated as the locations of the highest peaks in the PTF-MUSIC spectrum. For each angle ϕ_k corresponding to the n signal arrivals, $k = 1, 2, \dots, n$, the polarization parameters of the respective source signal can be estimated from

$$\hat{\mathbf{c}}(\phi_k) = \mathbf{v}_{\min} [\mathbf{F}^H(\phi_k)\mathbf{U}_n\mathbf{U}_n^H\mathbf{F}(\phi_k)], \quad (36)$$

where $\mathbf{v}_{\min}[\cdot]$ is the eigenvector corresponding to the minimum eigenvalue $\lambda_{\min}[\cdot]$.

V. SPATIO-POLARIMETRIC CORRELATIONS

The spatial resolution capability of an array highly depends on the correlation between the propagation signatures of the source arrivals [4], [31]. This is determined by the normalized inner product of the respective array manifold vectors. In the underlying problem, in which both the spatial and polarimetric dimensions are involved, the joint spatio-polarimetric correlation coefficient between sources l and k is defined using the extended array manifold $\tilde{\mathbf{a}}(\phi)$, i.e.,

$$\begin{aligned} \beta_{l,k} &= \frac{1}{m} \tilde{\mathbf{a}}^H(\phi_k) \tilde{\mathbf{a}}(\phi_l) \\ &= \frac{1}{m} \left(c_{k1}^* c_{l1} \left(\mathbf{a}^{[v]}(\phi_k) \right)^H \mathbf{a}^{[v]}(\phi_l) \right. \\ &\quad \left. + c_{k2}^* c_{l2} \left(\mathbf{a}^{[h]}(\phi_k) \right)^H \mathbf{a}^{[h]}(\phi_l) \right) \\ &= c_{k1}^* c_{l1} \beta_{l,k}^{[v]} + c_{k2}^* c_{l2} \beta_{l,k}^{[h]} \end{aligned} \quad (37)$$

where $\beta_{l,k}^{[i]} = (1/m)(\mathbf{a}^{[i]}(\phi_k))^H \mathbf{a}^{[i]}(\phi_l)$ is the spatial correlation coefficient between sources l and k for polarization i , with $i = v$ or h .

An interesting case arises when the vertically and horizontally polarized array manifolds are identical, i.e., $\mathbf{a}^{[v]}(\phi) =$

$\mathbf{a}^{[h]}(\phi)$. In this case, $\beta_{l,k}^{[v]} = \beta_{l,k}^{[h]}$, and the joint spatio-polarimetric correlation coefficient becomes the product of the individual spatial and polarimetric correlations, that is

$$\beta_{l,k} = \beta_{l,k}^{[v]} \rho_{l,k} \quad (38)$$

with

$$\rho_{l,k} = \mathbf{c}_k^H \mathbf{c}_l = \cos(\gamma_l) \cos(\gamma_k) e^{j(\eta_l - \eta_k)} + \sin(\gamma_l) \sin(\gamma_k) \quad (39)$$

representing the polarimetric correlation coefficient. In particular, for linear polarizations, $\eta_l = \eta_k = 0$, and (39) reduces to

$$\rho_{l,k} = \cos(\gamma_l - \gamma_k). \quad (40)$$

Since $|\rho_{l,k}| \leq 1$, with the equality holds only when the two sources have identical polarization states, the spatio-polarization correlation coefficient is always smaller than that of the individual spatial correlation coefficient. The reduction in the correlation value due to polarization diversity, through the introduction of $\rho_{l,m}$, translates to improved source distinctions. As such, two sources that could be difficult to resolve using the single-polarized spatial array manifold $\mathbf{a}^{[v]}(\phi)$ or $\mathbf{a}^{[h]}(\phi)$ can be easily separated using the extended spatio-polarized array manifold, defined by $\tilde{\mathbf{a}}(\phi)$. This improvement is more evident in the case when the source spatial correlation is high, but the respective polarimetric correlation is low.

VI. SOURCES WITH TIME-VARYING POLARIZATIONS

In this section, we consider the performance of DOA estimation when the source signals have time-varying polarization signatures. Time-varying polarizations are often observed when active or passive sources move or change orientations [32]. The performance of polarimetric MUSIC and PTF-MUSIC techniques are discussed and compared. For simplicity, we consider in this section the noise-free environment.

A. Polarimetric MUSIC

Given the time-varying nature of the source signal polarizations, the covariance matrix of the received signal vector is

$$\begin{aligned} \mathbf{R}_{\mathbf{xx}} &= E [\mathbf{x}(t)\mathbf{x}^H(t)] \\ &= E \left\{ \begin{bmatrix} \mathbf{A}^{[v]}(\Phi) (\mathbf{q}^{[v]}(t) \odot \mathbf{s}(t)) \\ \mathbf{A}^{[h]}(\Phi) (\mathbf{q}^{[h]}(t) \odot \mathbf{s}(t)) \end{bmatrix} \right. \\ &\quad \left. \times \begin{bmatrix} \mathbf{A}^{[v]}(\Phi) (\mathbf{q}^{[v]}(t) \odot \mathbf{s}(t)) \\ \mathbf{A}^{[h]}(\Phi) (\mathbf{q}^{[h]}(t) \odot \mathbf{s}(t)) \end{bmatrix}^H \right\}. \end{aligned} \quad (41)$$

We replace the expectation operator by time-averages. Then, we have (42), shown at the bottom of the page, where $\overline{(\cdot)}$ denotes the average and $\hat{\mathbf{R}}_{\mathbf{ss}}$ is the time-average estimate of the source

$$\begin{aligned} \mathbf{R}_{\mathbf{xx}} &= \mathbf{B}(\Phi) \begin{bmatrix} \overline{\mathbf{q}^{[v]}(t) (\mathbf{q}^{[v]}(t))^H} \odot \hat{\mathbf{R}}_{\mathbf{ss}} & \overline{\mathbf{q}^{[v]}(t) (\mathbf{q}^{[h]}(t))^H} \odot \hat{\mathbf{R}}_{\mathbf{ss}} \\ \overline{\mathbf{q}^{[h]}(t) (\mathbf{q}^{[v]}(t))^H} \odot \hat{\mathbf{R}}_{\mathbf{ss}} & \overline{\mathbf{q}^{[h]}(t) (\mathbf{q}^{[h]}(t))^H} \odot \hat{\mathbf{R}}_{\mathbf{ss}} \end{bmatrix} \mathbf{B}^H(\Phi) \\ &= \mathbf{B}(\Phi) \left\{ \begin{bmatrix} \overline{\mathbf{q}^{[v]}(t) (\mathbf{q}^{[v]}(t))^H} & \overline{\mathbf{q}^{[v]}(t) (\mathbf{q}^{[h]}(t))^H} \\ \overline{\mathbf{q}^{[h]}(t) (\mathbf{q}^{[v]}(t))^H} & \overline{\mathbf{q}^{[h]}(t) (\mathbf{q}^{[h]}(t))^H} \end{bmatrix} \odot \begin{bmatrix} \hat{\mathbf{R}}_{\mathbf{ss}} & \hat{\mathbf{R}}_{\mathbf{ss}} \\ \hat{\mathbf{R}}_{\mathbf{ss}} & \hat{\mathbf{R}}_{\mathbf{ss}} \end{bmatrix} \mathbf{B}^H(\Phi) \right\}. \end{aligned} \quad (42)$$

covariance matrix. The time-varying source signal polarization vectors are defined, similarly to (26) and (27), as

$$\mathbf{q}^{[v]}(t) = [\cos(\gamma_1(t)), \dots, \cos(\gamma_n(t))]^T \quad (43)$$

$$\mathbf{q}^{[h]}(t) = [\sin(\gamma_1(t))e^{j\mathcal{M}_1(t)}, \dots, \sin(\gamma_n(t))e^{j\mathcal{M}_n(t)}]^T. \quad (44)$$

If the source signal polarizations assume constant values, i.e., $\mathbf{q}^{[v]}(t) = \mathbf{q}^{[v]}$ and $\mathbf{q}^{[h]}(t) = \mathbf{q}^{[h]}$, then the noise-free received signal covariance matrix becomes

$$\mathbf{R}'_{\mathbf{xx}} = \mathbf{B}(\Phi) \left(\begin{bmatrix} \mathbf{q}^{[v]} (\mathbf{q}^{[v]})^H & \mathbf{q}^{[v]} (\mathbf{q}^{[h]})^H \\ \mathbf{q}^{[h]} (\mathbf{q}^{[v]})^H & \mathbf{q}^{[h]} (\mathbf{q}^{[h]})^H \end{bmatrix} \odot \begin{bmatrix} \mathbf{R}_{\text{ss}} & \mathbf{R}_{\text{ss}} \\ \mathbf{R}_{\text{ss}} & \mathbf{R}_{\text{ss}} \end{bmatrix} \right) \mathbf{B}^H(\Phi). \quad (45)$$

The effect of the signal time-varying polarization on the covariance matrix is evident from (42) and (45). The two cases of time-varying and time-invariant polarizations will lead to the same performance if their corresponding covariance matrices are identical. Consider, for example, a covariance matrix due to two source signals. The first signal has a linearly time-varying polarization over the observation period from 0° to 90° , whereas the second signal's linear polarization varies from 90° to 0° over the same period. This case is equivalent to both sources assuming fixed, time-invariant polarization of $\gamma = 45^\circ$, and thereby, the source polarization diversity cannot be utilized in DOA estimation using polarimetric MUSIC.

To achieve polarization diversity in the above case, the data covariance matrix in (42) should be constructed from the moving average of the received data vector, instead of averaging over the entire data record. However, using few samples compromises the precision and robustness of direction estimation.

B. PTF-MUSIC

In the presence of time-varying polarized sources, the auto- and cross-polarized SPTFD, defined in (19) and (21), respectively, can be expressed as

$$\begin{aligned} \mathbf{D}_{\mathbf{x}^{[i]}\mathbf{x}^{[j]}}(t, f) &= \iint \varphi(t-u, \tau) \mathbf{x}^{[i]} \left(u + \frac{\tau}{2}\right) \left(\mathbf{x}^{[j]} \left(u - \frac{\tau}{2}\right)\right)^H e^{-j2\pi f\tau} dud\tau \\ &= \mathbf{A}^{[i]}(\Phi) \\ &\quad \times \left[\iint \varphi(t-u, \tau) \left(\mathbf{q}^{[i]} \left(u + \frac{\tau}{2}\right)\right) \left(\mathbf{q}^{[j]} \left(u - \frac{\tau}{2}\right)\right)^H \right. \\ &\quad \left. \odot \left(\mathbf{s} \left(u + \frac{\tau}{2}\right)\mathbf{s}^H \left(u - \frac{\tau}{2}\right)\right) e^{-j2\pi f\tau} dud\tau \right] \left(\mathbf{A}^{[j]}(\Phi)\right)^H \\ &= \mathbf{A}^{[i]}(\Phi) \left[\iint \varphi(t-u, \tau) \mathbf{G}^{[ij]}(u, \tau) \right. \\ &\quad \left. \odot \mathbf{K}(u, \tau) e^{-j2\pi f\tau} dud\tau \right] \left(\mathbf{A}^{[j]}(\Phi)\right)^H \\ &= \mathbf{A}^{[i]}(\Phi) \mathbf{D}_{\mathbf{s}^{[i]}\mathbf{s}^{[j]}}(t, f) \left(\mathbf{A}^{[j]}(\Phi)\right)^H \end{aligned} \quad (46)$$

where $\mathbf{G}^{[ij]}(t, \tau) = \mathbf{q}^{[i]}(t + (\tau/2))(\mathbf{q}^{[j]}(t - (\tau/2)))^H$, and $\mathbf{K}(t, \tau) = \mathbf{s}(t + (\tau/2))\mathbf{s}^H(t - (\tau/2))$. We assume that the frequency and the polarization signatures of the sources change almost linearly within the temporal span

of the t-f kernel. Then, using the first-order Taylor-series expansion, the polarization-dependent terms can be approximated as $\gamma_k(t + (\tau/2)) = \gamma_k(t) + (\tau/2)\dot{\gamma}_k(t)$, where $\dot{\gamma}_k(t) = (d/dt)\gamma_k(t)$. The autoterms of the source polarization information, which reside on the diagonals of $\mathbf{G}^{[vv]}(t, \tau)$, $\mathbf{G}^{[vh]}(t, \tau)$, $\mathbf{G}^{[hv]}(t, \tau)$ and $\mathbf{G}^{[hh]}(t, \tau)$, are given by

$$\left[\mathbf{G}^{[vv]}(t, \tau)\right]_{kk} = \frac{1}{2} [\cos(2\gamma_k(t)) + \cos(\tau\dot{\gamma}_k(t))] \quad (47)$$

$$\left[\mathbf{G}^{[vh]}(t, \tau)\right]_{kk} = \frac{1}{2} [\sin(2\gamma_k(t)) - \sin(\tau\dot{\gamma}_k(t))] \quad (48)$$

$$\left[\mathbf{G}^{[hv]}(t, \tau)\right]_{kk} = \frac{1}{2} [\sin(2\gamma_k(t)) + \sin(\tau\dot{\gamma}_k(t))] \quad (49)$$

$$\left[\mathbf{G}^{[hh]}(t, \tau)\right]_{kk} = \frac{1}{2} [-\cos(2\gamma_k(t)) + \cos(\tau\dot{\gamma}_k(t))] \quad (50)$$

respectively. For symmetric t-f kernels, $\varphi(t, \tau)$, the second sinusoidal terms in (48) and (49) assume zero values in the TFD. Therefore, $\mathbf{D}_{\mathbf{s}^{[i]}\mathbf{s}^{[j]}}(t, f)$ can be expressed at the autoterm points as

$$D_{s_k^{[v]}s_k^{[v]}}(t, f) = \frac{1}{2} \cos(2\gamma_k(t)) D_{s_k s_k}(t, f) + c_{kk}(t, f) \quad (51)$$

$$D_{s_k^{[h]}s_k^{[h]}}(t, f) = -\frac{1}{2} \cos(2\gamma_k(t)) D_{s_k s_k}(t, f) + c_{kk}(t, f) \quad (52)$$

$$\begin{aligned} D_{s_k^{[v]}s_k^{[h]}}(t, f) &= D_{s_k^{[h]}s_k^{[v]}}(t, f) \\ &= \frac{1}{2} \sin(2\gamma_k(t)) D_{s_k s_k}(t, f) \end{aligned} \quad (53)$$

with

$$c_{kk}(t, f) = \frac{1}{2} \iint \cos(\tau\dot{\gamma}_k(t)) \varphi(t-u, \tau) \times [\mathbf{K}(t, \tau)]_{kk} e^{-j2\pi f\tau} dud\tau. \quad (54)$$

When different sources are uncorrelated, their time-frequency signatures have no significant overlap. If the t-f points located in the autoterm region of the k th source are used in constructing the SPTFD matrix, then

$$\begin{aligned} \mathbf{D}_{\mathbf{xx}}(t, f) &= \begin{bmatrix} \mathbf{a}^{[v]}(\phi_k) & 0 \\ 0 & \mathbf{a}^{[h]}(\phi_k) \end{bmatrix} \\ &\quad \times \mathbf{M}_k \begin{bmatrix} \mathbf{a}^{[v]}(\phi_k) & 0 \\ 0 & \mathbf{a}^{[h]}(\phi_k) \end{bmatrix}^H \end{aligned} \quad (55)$$

where

$$\begin{aligned} \mathbf{M}_k &= \frac{1}{2} D_{s_k s_k}(t, f) \begin{bmatrix} \cos(2\gamma_k(t)) & \sin(2\gamma_k(t)) \\ \sin(2\gamma_k(t)) & -\cos(2\gamma_k(t)) \end{bmatrix} \\ &\quad + \begin{bmatrix} c_{kk}(t, f) & 0 \\ 0 & c_{kk}(t, f) \end{bmatrix}. \end{aligned}$$

In the new structure of the SPTFD matrix of (55), the source time-varying polarization has the effect of loading the diagonal elements with $c_{kk}(t, f)$ and, as such, alters the eigenvalues of the above 2×2 matrix. However, the eigenvector of \mathbf{M}_k remain unchanged. The new eigenvalues are $\lambda_{1,2} = c_{kk}(t, f) \pm (1/2)D_{s_k s_k}(t, f)$. The signal polarization signature, i.e., the eigenvector corresponding to the maximum eigenvalue, is $\mathbf{v}_{k, \max} = [\cos(\gamma_k(t)) \sin(\gamma_k(t))]^T$. Therefore,

TABLE I
 SIGNAL PARAMETERS (UNCORRELATED SOURCE SCENARIO)

	start	end	DOA	γ	η
	freq.	freq.	(deg.)	(deg.)	(deg.)
source 1	0.20	0.40	-3	45	0
source 2	0.22	0.42	3	45	180
source 3	0.10	0.10	9	20	0

in the context of PTF-MUSIC, the instantaneous polarization characteristics can be utilized for source discriminations.

VII. SUBARRAY AND POLARIMETRIC AVERAGING

In coherent signal environments, spatial smoothing [28] and polarization averaging [29] methods are commonly applied in the MUSIC algorithms to restore the rank of the source matrix, prior to signal and noise subspace estimations. While spatial smoothing has a drawback of reducing the array aperture, polarization averaging eliminates pertinent source polarization information. In a combined spatial and polarization averaging approach, signal polarizations can be used to limit the reduction in array aperture. This, in turn, increases the number of coherent sources that can be resolved by the array over the case where only spatial averaging is performed.

In this section, the above methods are considered for the PTF-MUSIC for estimating DOAs of coherent sources in the context of TFDs, using dual-polarized double-feed arrays. For subarray averaging, uniform linear arrays (ULAs) are assumed with identical array manifolds for both polarizations, i.e., $\mathbf{a}^{[v]}(\phi) = \mathbf{a}^{[h]}(\phi) = \mathbf{a}(\phi)$. For polarization averaging, only the latter assumption (identical manifolds for both polarizations) is required.

A. Subarray Averaging

Subarray averaging involves dividing the m dual-polarized antenna array into p overlapping subarrays of $m_1 = m - p + 1$ antennas, and averaging the respective p subarray SPTFD matrices. Define $\mathbf{A}_1(\Phi)$ as the new $m_1 \times n$ steering matrix for the first subarray which consists of the first m_1 rows of matrix $\mathbf{A}(\Phi) = \mathbf{A}^{[v]}(\Phi) = \mathbf{A}^{[h]}(\Phi)$. The data vector at the k th subarray is expressed as

$$\begin{aligned} \mathbf{x}^{(k)}(t) &= \begin{bmatrix} \mathbf{x}^{(k)[v]}(t) \\ \mathbf{x}^{(k)[h]}(t) \end{bmatrix} \\ &= \mathbf{B}_1^{(k)}(\Phi) \begin{bmatrix} \mathbf{s}^{[v]}(t) \\ \mathbf{s}^{[h]}(t) \end{bmatrix} + \begin{bmatrix} \mathbf{n}^{(k)[v]}(t) \\ \mathbf{n}^{(k)[h]}(t) \end{bmatrix}, \quad k = 1, 2, \dots, m_1 \end{aligned} \quad (56)$$

where $\mathbf{n}^{(k)[i]}(t)$ is the noise vector at the subarray for polarization i , $i = v$ or h

$$\mathbf{B}_1^{(k)}(\Phi) = \begin{bmatrix} \mathbf{A}_1(\Phi)\mathbf{\Lambda}^{k-1}(\Phi) & \mathbf{0} \\ \mathbf{0} & \mathbf{A}_1(\Phi)\mathbf{\Lambda}^{k-1}(\Phi) \end{bmatrix} \quad (57)$$

$$\mathbf{\Lambda}(\Phi) = \text{diag} \left[e^{-j2\pi \frac{d}{\lambda} \sin(\phi_1)}, \dots, e^{-j2\pi \frac{d}{\lambda} \sin(\phi_n)} \right] \quad (58)$$

where d denotes the sensor interelement spacing and λ denotes the source wavelength. Denoting $\mathbf{D}_{\mathbf{x}\mathbf{x}}^{(k)}(t, f)$ as the SPTFD matrix corresponding to $\mathbf{x}^{(k)}(t)$ of the k th subarray, the spatially smoothed SPTFD matrix is defined by averaging $\mathbf{D}_{\mathbf{x}\mathbf{x}}^{(k)}(t, f)$ over the p subarrays, i.e.,

$$\mathbf{D}_{\mathbf{x}\mathbf{x}SA}(t, f) = \frac{1}{p} \sum_{k=1}^p \mathbf{D}_{\mathbf{x}\mathbf{x}}^{(k)}(t, f). \quad (59)$$

The averaged SPTFD matrix can be written as the augmentation of four spatially-smoothed auto- and cross-polarized SPTFD matrices, expressed as

$$\mathbf{D}_{\mathbf{x}\mathbf{x}SA}(t, f) = \begin{bmatrix} \mathbf{D}_{\mathbf{x}\mathbf{x}SA}^{[vv]}(t, f) & \mathbf{D}_{\mathbf{x}\mathbf{x}SA}^{[vh]}(t, f) \\ \mathbf{D}_{\mathbf{x}\mathbf{x}SA}^{[hv]}(t, f) & \mathbf{D}_{\mathbf{x}\mathbf{x}SA}^{[hh]}(t, f) \end{bmatrix}. \quad (60)$$

The (k, l) -th element of $\mathbf{D}_{\mathbf{x}\mathbf{x}SA}^{[ij]}(t, f)$, $i, j = v, h$, with $k, l = 1, 2, \dots, m_1$, of the auto- ($i = j$) and cross-polarized ($i \neq j$) matrices in the above equation can be described as

$$\begin{aligned} D_{x_k x_l SA}^{[ij]}(t, f) &= \frac{1}{p} \sum_{r=1}^p D_{x_{k+r-1} x_{l+r-1}}^{[ij]}(t, f) \\ &= \frac{1}{p} \sum_{r=1}^p \left(\sum_{b=1}^n \sum_{c=1}^n a_{b, k+r-1} (a_{c, l+r-1})^* D_{s_b s_c}^{[ij]}(t, f) \right) \\ &= \sum_{b=1}^n \sum_{c=1}^n \left(\frac{1}{p} \sum_{r=1}^p a_{b, k+r-1} (a_{c, l+r-1})^* \right) D_{s_b s_c}^{[ij]}(t, f) \\ &= \sum_{b=1}^n \sum_{c=1}^n \left(\frac{1}{p} \check{\mathbf{a}}_{c, k}^H \check{\mathbf{a}}_{b, l} \right) D_{s_b s_c}^{[ij]}(t, f) \\ &= \sum_{b=1}^n \sum_{c=1}^n \check{\beta}_{b, c, k, l} D_{s_b s_c}^{[ij]}(t, f) \end{aligned} \quad (61)$$

where $\check{\mathbf{a}}_{b, l} = [e^{-j2\pi(l-1)(d/\lambda)\sin(\theta_b)}, e^{-j2\pi l(d/\lambda)\sin(\theta_b)}, \dots, e^{-j2\pi(l+p-2)(d/\lambda)\sin(\theta_b)}]^T$ is the steering vector of a subgroup of p sensors for which the received signals are averaged, and $\check{\beta}_{b, c, k, l} = \check{\mathbf{a}}_{c, k}^H \check{\mathbf{a}}_{b, l} / p$ is the spatial correlation between signals b and c defined in the p -sensor group. It is easy to show that $|\check{\beta}_{b, b, k, l}| = 1$ for any b , whereas $|\check{\beta}_{b, c, k, l}| < 1$ for $b \neq c$. Different values of k and l affect the phase of $|\check{\beta}_{b, c, k, l}|$ but not its magnitude. Therefore, averaging the TFDs of the received data across the p array sensors reduces the interactions between source signals, whereas the source autoterms remain unchanged. This in turn reduces the off-diagonal elements of

the source TFD matrix $\mathbf{D}_{ss}(t, f)$ and leads to matrix rank restoration.

B. Polarimetric Averaging

Similar to subarray averaging, polarimetric averaging aims at combating the rank deficiency of the source SPTFD matrix, $\mathbf{D}_{ss}(t, f)$, provided that the sources have different polarization states. The polarimetric averaged SPTFD matrix is defined as

$$\mathbf{D}_{xxPA}(t, f) = \frac{1}{2} [\mathbf{D}_{\mathbf{x}^{[v]}\mathbf{x}^{[v]}}(t, f) + \mathbf{D}_{\mathbf{x}^{[h]}\mathbf{x}^{[h]}}(t, f)]. \quad (62)$$

As with subarray averaging, polarization averaging also reduces source signal crossterms depending on the polarization correlation between them, as was shown in [33].

C. Combined Spatial and Polarimetric Averaging

Polarization averaging can also be used in conjunction with subarray averaging. Denote $\mathbf{D}_{\mathbf{x}^{[v]}\mathbf{x}^{[v]}}^{(k)}(t, f)$ and $\mathbf{D}_{\mathbf{x}^{[h]}\mathbf{x}^{[h]}}^{(k)}(t, f)$ as the STFDs corresponding to $\mathbf{x}^{(k)[v]}(t)$ and $\mathbf{x}^{(k)[h]}(t)$, respectively. Then, the combined subarray and polarization averaged SPTFD matrix becomes

$$\mathbf{D}_{xxSPA}(t, f) = \frac{1}{2p} \sum_{k=1}^p [\mathbf{D}_{\mathbf{x}^{[v]}\mathbf{x}^{[v]}}^{(k)}(t, f) + \mathbf{D}_{\mathbf{x}^{[h]}\mathbf{x}^{[h]}}^{(k)}(t, f)]. \quad (63)$$

It is implicit in (59)–(63) that whether it is polarization and/or subarray averaging, source decorrelation is performed for each t-f point. Once the rank deficiency in the SPTFD matrices corresponding to multiple t-f points is restored, one can estimate the DOAs through PTF-MUSIC (for subarray averaging) or TF-MUSIC (for polarimetric or combined spatial and polarimetric averaging since the polarimetric information is lost in the process of averaging).

D. Decorrelation Requirements

Consider that n_0 sources are selected in the t-f domain, out of which a maximum number of n_c sources are coherent with each other. It is well-known that to decorrelate n_c coherent sources using spatial averaging, the minimum number of subarrays must be $p \geq n_c$. In addition, the condition $m_1 > n_0$ is required so that the DOAs of all n_0 sources can be identified. However, when polarization averaging is used in addition to subarray averaging, only half the number of subarrays is needed, i.e., $p \geq \lceil n_c/2 \rceil$, given that the polarization states of the coherent sources are not identical. Accordingly, to decorrelate two coherent sources with different polarization states, polarization averaging alone will suffice. To decorrelate four coherent sources with different polarization states, polarization averaging accompanied with two subarrays will then be required. The proof of the reduction of the number of subarrays in the presence of polarization averaging was provided in [29] for non-time-frequency-based methods. The extension to the t-f based methods is rather straightforward, and achieved by substituting the covariance matrix with a STFD or SPTFD matrix [34].

E. Remarks

From the above discussion, the following remarks are in order.

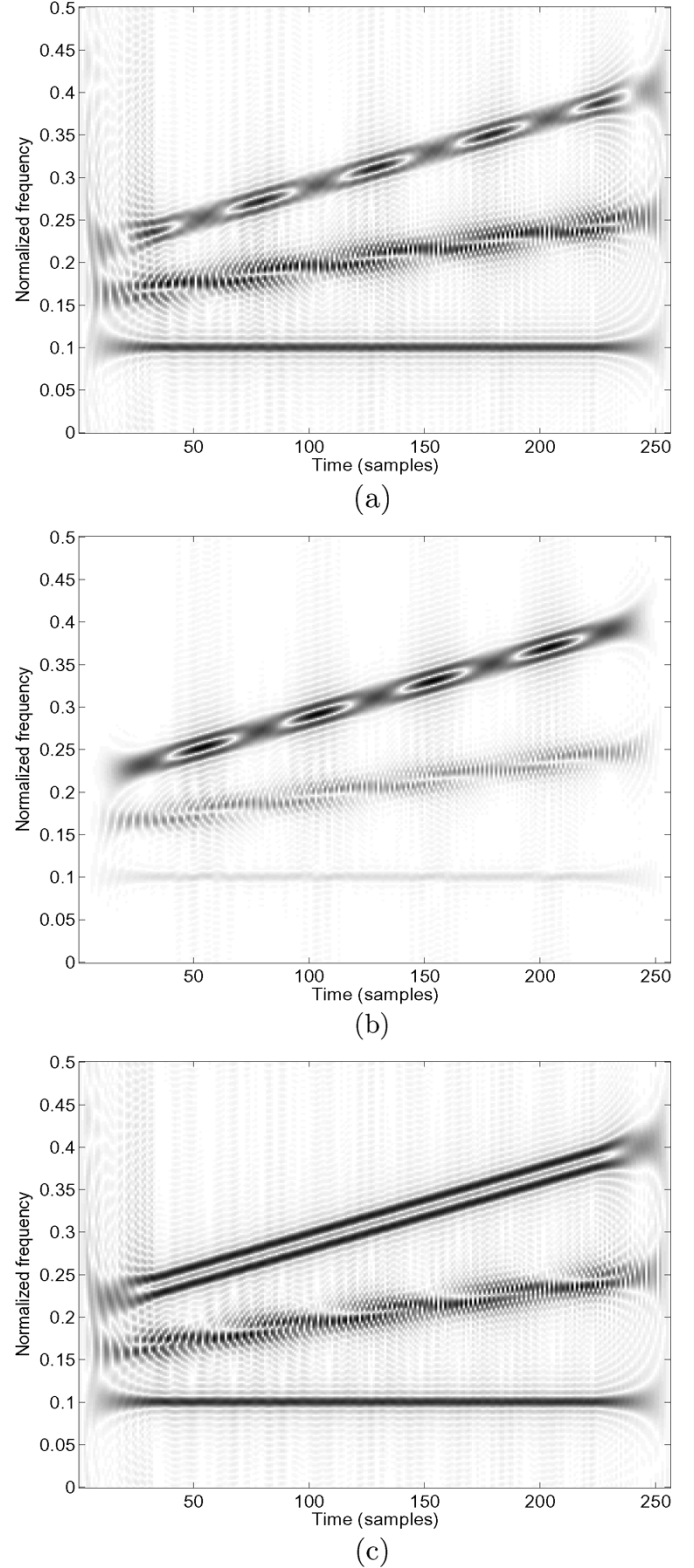


Fig. 2. Averaged PWVD results. (a) PWVD averaged over the vertically-polarized array sensors; (b) PWVD averaged over the horizontally-polarized array sensors; and (c) PWVD averaged over array sensors and polarizations.

- 1) Polarization averaging does not require a ULA, a condition that has to be satisfied in subarray averaging. However, the dual-polarized sensors must be identically po-

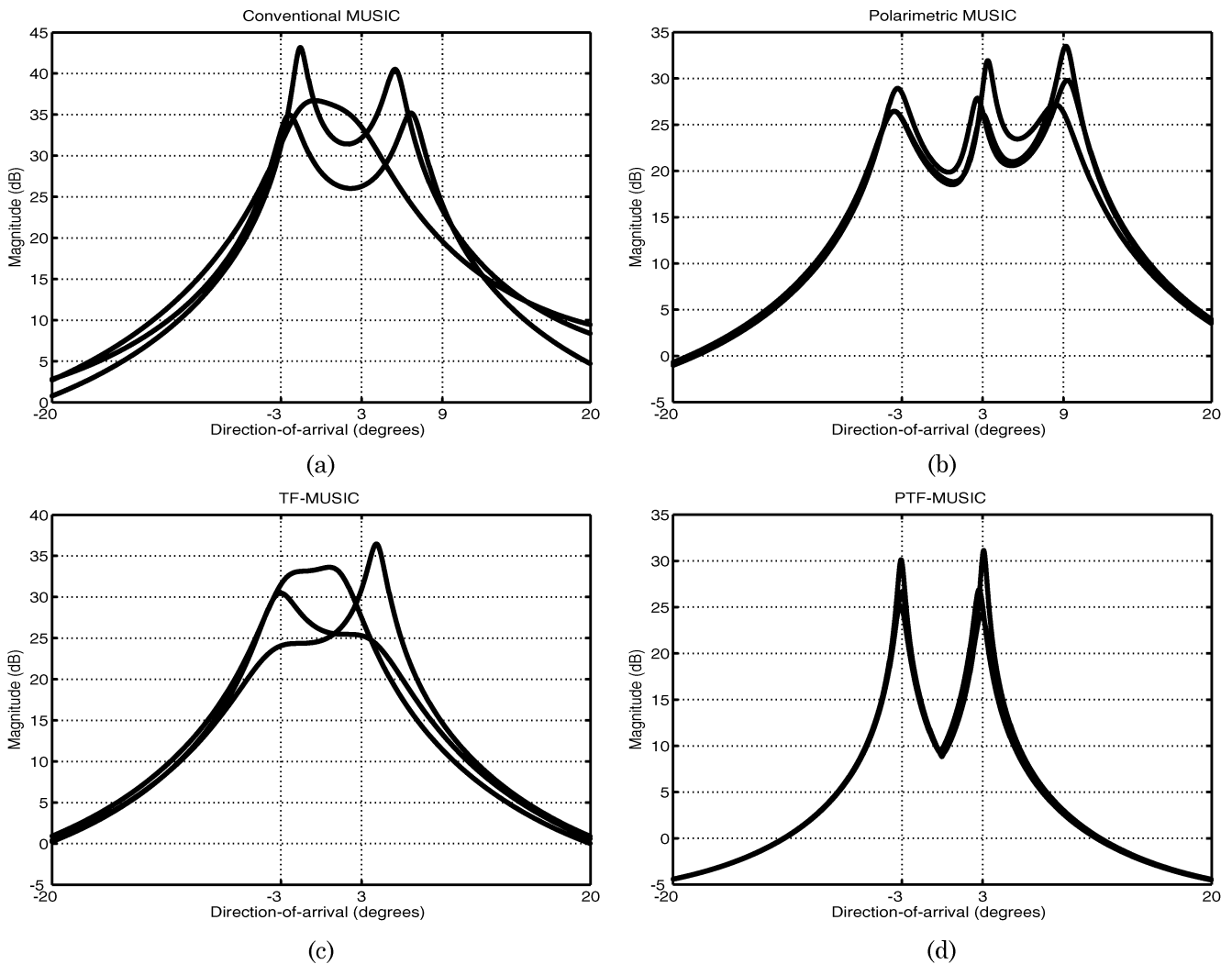


Fig. 3. Comparison of MUSIC spectra: (a) Conventional MUSIC; (b) polarimetric MUSIC; (c) TF-MUSIC; and (d) PTF-MUSIC.

larized and both polarizations have the identical array manifolds.

- 2) Polarization averaging is beneficial for matrix rank restoration only when the coherent sources have different polarization states. Polarization averaging sacrifices the polarization information and, therefore, signal polarization parameters can not be estimated.
- 3) In some cases, polarization averaging must be utilized along with subarray averaging. For example, when three sources impinge on a five-sensors ULA, while polarization averaging combined with two subarrays can resolve the source DOAs, subarray averaging alone would fail.

VIII. SIMULATIONS

A. Uncorrelated Source Scenarios

We consider two sources (sources 1 and 2) with chirp waveforms in the presence of an undesired sinusoidal signal (source 3) which impinge on a ULA of four ($m = 4$) dual-polarized cross-dipoles with half-wavelength interelement spacing. The

vertical and horizontal array manifolds are set to be equal. Table I shows the sources' respective normalized starting and end frequencies, DOAs (measured from the broadside), and the two polarization parameters, γ and η . All signals have the same signal power (SNR = 13 db). The task is to find the DOAs of the chirp signals. The data length is 256 samples and the length of the rectangular window used in the pseudo Wigner–Ville distribution (PWVD) is 65 samples.

As proposed in [35], averaging the sensor TFDs across the array mitigates the source cross terms and, as such, enhances the source t-f signatures. The PWVDs averaged over the four sensors are shown in Fig. 2(a) and (b), respectively, for the vertical and horizontal polarizations. Because the sources are closely spaced, crossterm mitigation through array averaging is limited. To further suppress the crossterms, we utilize both the spatial and polarimetric dimensions. Fig. 2(c) shows the PWVD averaged over the four sensors as well as both polarizations. In this case, since source 1 and source 2 have orthogonal polarizations, the cross terms between the two chirp signals are completely suppressed, revealing the source instantaneous frequencies and the true chirp signatures. The t-f points along these signatures

TABLE II
SIGNAL PARAMETERS (COHERENT SOURCE SCENARIO)

	start	end	DOA	γ	η
	freq.	freq.	(deg.)	(deg.)	(deg.)
source 1	0.20	0.50	-6	35	5
source 2	0.20	0.50	6	45	170
source 3	0.10	0.10	12	25	-90

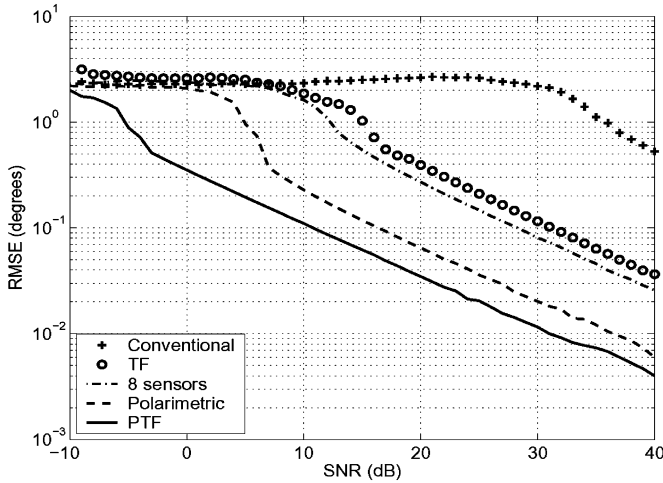


Fig. 4. RMSE performance of the MUSIC methods.

can, subsequently, be considered for STFD and SPTFD matrix constructions.

The PTF-MUSIC spectrum is computed and the results are compared with the conventional MUSIC, polarimetric MUSIC, and TF-MUSIC. The MUSIC spectra for three independent trials are shown in Fig. 3. For the conventional and TF-MUSIC, only the vertical polarization components are used. For the TF- and the PTF-MUSIC, 192 t-f points were selected along the signatures of each of the two chirp signals meanwhile the sinusoidal signal is eliminated from consideration. The TF-MUSIC benefits from fewer sources and increased SNR, whereas the polarimetric MUSIC utilizes the distinction in the source polarization properties. Both attributes are enjoyed by the PTF-MUSIC. It is evident that only the proposed PTF-MUSIC accurately estimates the DOAs of the two chirp sources.

Fig. 4 shows the root mean square error (RMSE) performance of estimated DOA for the four MUSIC methods. The results are obtained using 50 independent trials for each value of SNR and averaged over all the selected sources. The RMSE performance of the conventional MUSIC with twice the number of sensors (i.e., eight sensors) is also included for comparison. It is seen that the PTF-MUSIC outperforms all other methods. The PTF-MUSIC enjoys about 5-dB gain over the polarimetric MUSIC due to the source selection/discrimination capability and the localization of the source signal energy.

B. Coherent Source Scenarios

In the second set of simulations, we consider a ULA of five ($m = 5$) dual-polarized cross-dipoles with half-wavelength interelement spacing. Three sources are considered. The first two

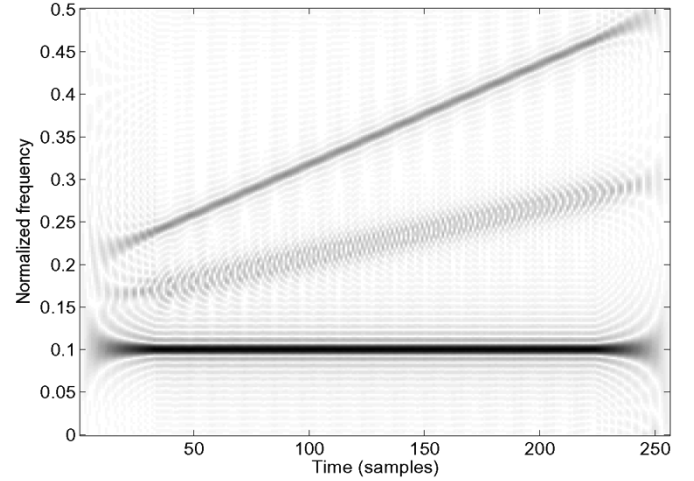


Fig. 5. PWVD averaged over all array sensors and polarizations.

sources (sources 1 and 2) are coherent and of identical chirp signatures, whereas the third one is an undesired sinusoidal signal (source 3). Table II shows the signal parameters. All signals have the same signal power (SNR = 10 dB). The data length is 256 samples. The PWVD averaged over the five dual-polarized sensors is shown in Fig. 5.

1) *Polarimetric Averaging*: Polarimetric averaging of the STFD matrices of the data samples across the vertical and the horizontal polarizations can successfully decorrelate coherent sources. Fig. 6 shows the spectra of the conventional MUSIC and TF-MUSIC, respectively, over three independent trials, where polarimetric averaging was employed on the five vertical and five horizontal antennas. For the TF-MUSIC method, only the two coherent sources (i.e., sources 1 and 2) are selected. It is evident that both methods show a clear spectrum peak for source 1 as a result of successful decorrelation of the two coherent sources. However, only the TF-MUSIC shows an exemplary performance for both sources due to the source selection capability.

2) *Subarray and Polarization Averaging*: In this simulation, polarimetric averaging is performed combined with spatial smoothing. The spectra of the MUSIC and the TF-MUSIC techniques utilizing the combined polarization and subarray averaging are shown in Fig. 7. In this case, the number of subarrays is 2. For comparison, we plotted in Fig. 8 the spectra using the conventional MUSIC method, applied to 10 vertically-polarized antenna array. Due to the close spatial separation between sources 2 and 3, the performance of all non-time-frequency-based methods is not satisfactory. Only the TF-MUSIC spectrum, which drops the third signal from

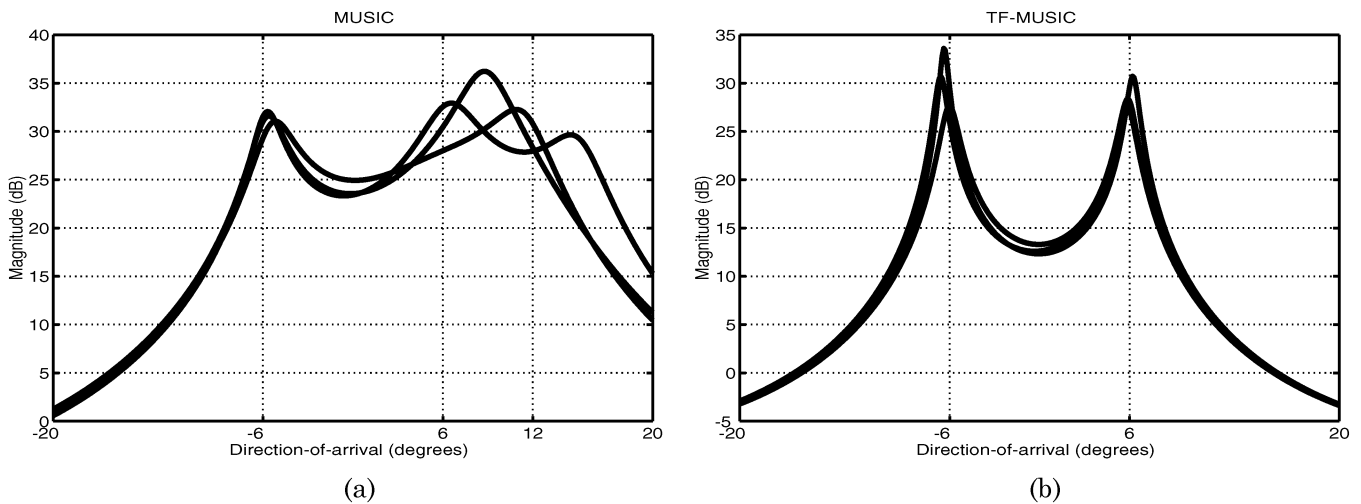


Fig. 6. Conventional MUSIC and TF-MUSIC spectra with polarization averaging: (a) Conventional MUSIC and (b) TF-MUSIC (two signals chosen).

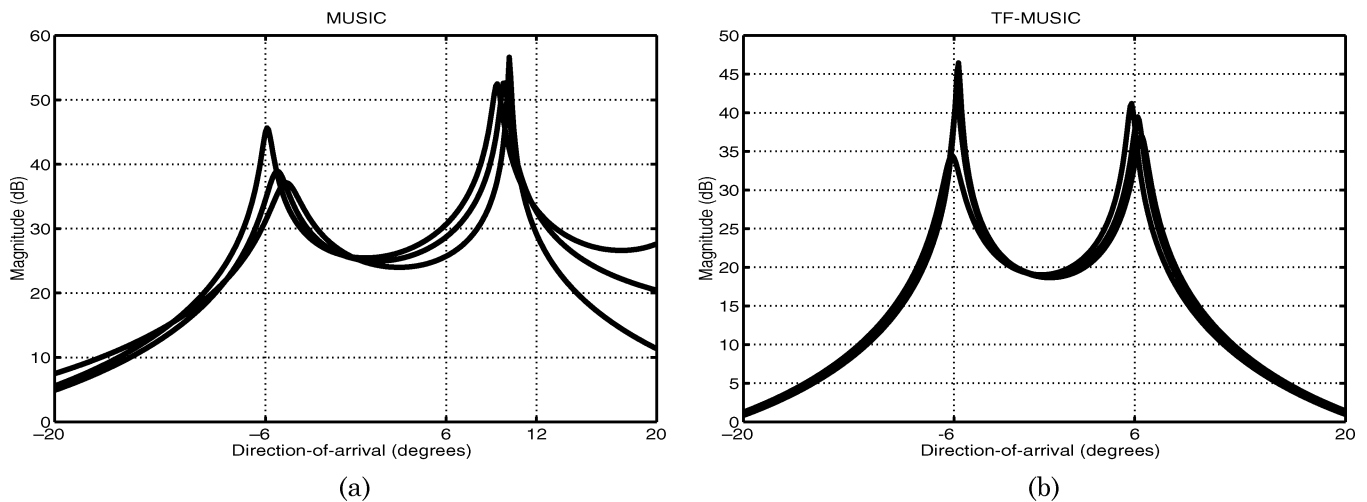


Fig. 7. Conventional and TF-MUSIC spectra with spatial smoothing and polarization averaging: (a) MUSIC and (b) TF-MUSIC (two signals chosen).

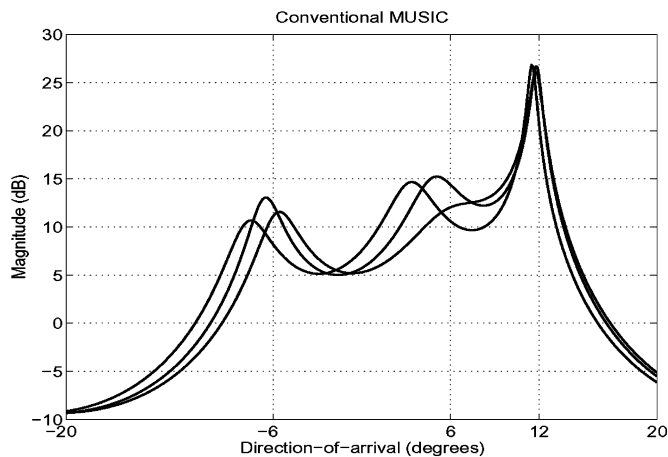


Fig. 8. Ten-sensor conventional MUSIC with spatial smoothing.

consideration, shows sharp and less biased peaks at the DOAs of the two coherent sources.

C. Sources With Time-Varying Polarization

Two chirp signals impinge upon a uniform linear array (ULA) of five cross-polarized (horizontal and vertical) dual-feed sensors. The parameters of the two chirp signals are listed in Table III. Fig. 9 shows the PWVD of two chirp signals. The interelement spacing of the sensors is half a wavelength. The array responses in both horizontal and vertical polarizations are identical. The SNR is 5 dB. The source signals' polarization angles $\gamma_1(t)$ and $\gamma_2(t)$ change linearly in the observation period of 512 samples and are shown in Fig. 10. The length of the rectangular window used in the PWVD is 65 samples.

We compare the spectra of polarimetric MUSIC and PTF-MUSIC algorithms, where the sources have time-dependent polarizations. When all data samples are used to construct the covariance matrix, polarimetric MUSIC estimation fails to resolve the two sources as both sources appear to have the same polarization [see Fig. 11(a)]. This is due to the fact that the two sources have the same second-order moment of the polarization

TABLE III
SIGNAL PARAMETERS (TIME-VARYING POLARIZATION SCENARIO)

	start	end	DOA	γ	η
	freq.	freq.	(deg.)	(deg.)	(deg.)
source 1	0.10	0.30	4	0 to 90	0
source 2	0.20	0.40	12	90 to 0	0

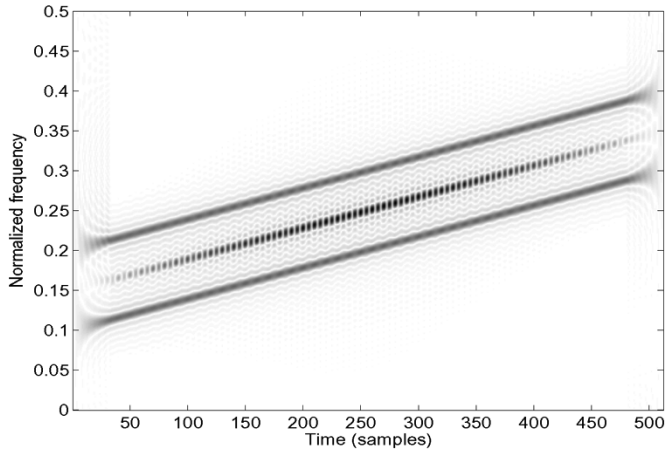
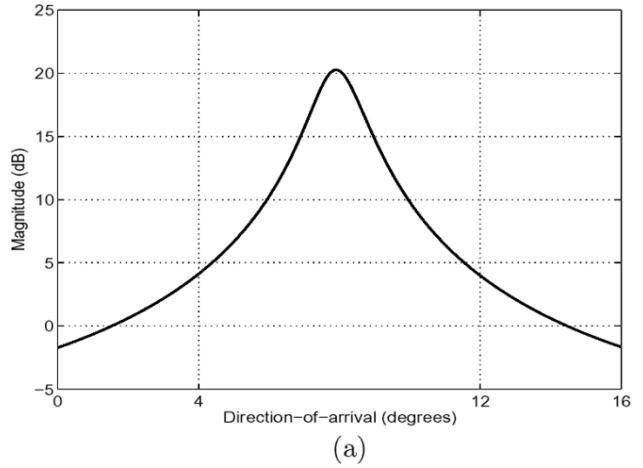


Fig. 9. PWVD of two chirp signals arriving at the reference sensor.



(a)

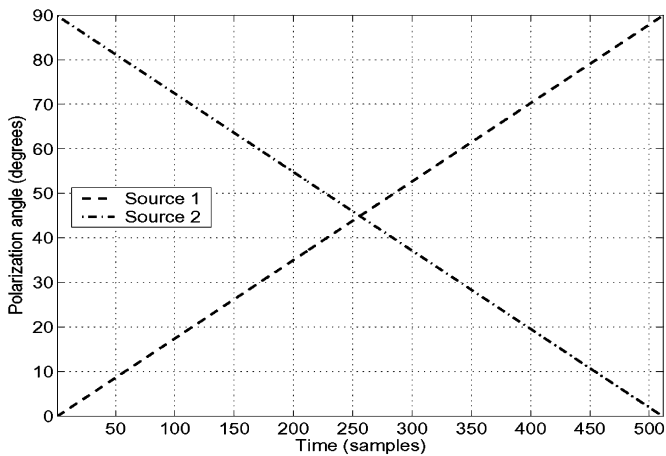
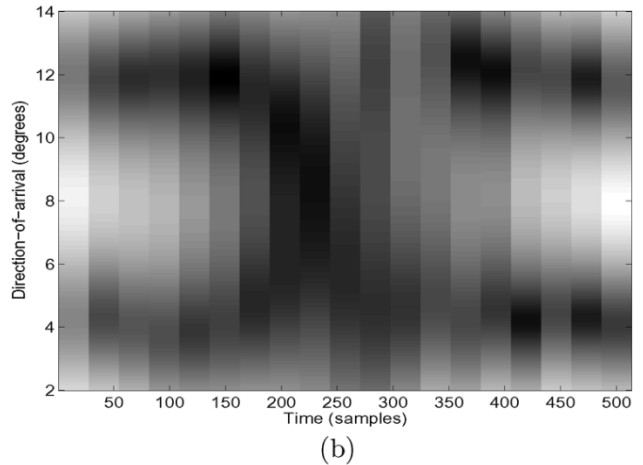
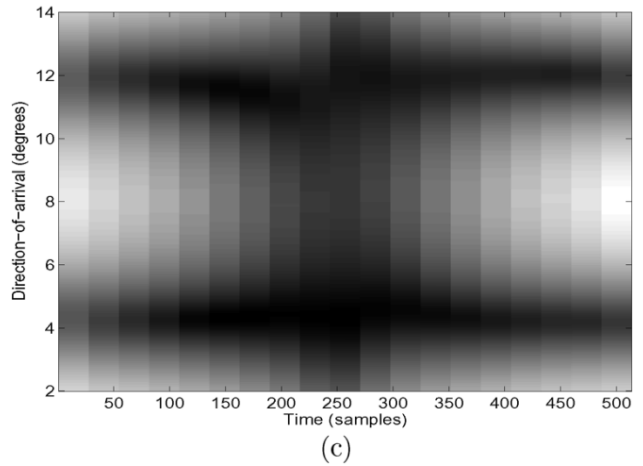


Fig. 10. Time-varying polarization signatures of the sources.



(b)



(c)

signature over the observation period and, therefore, the covariance matrix based polarimetric MUSIC method cannot distinguish their instantaneous polarization differences.

To take advantage of the time-varying polarizations, therefore, we use 95 snapshots in constructing the covariance matrix for the polarimetric MUSIC in a moving averaging scheme, whereas 95 consecutive t-f points are used for the PTF-MUSIC. Fig. 11(b) and (c) shows the performance of the polarimetric MUSIC and PTF-MUSIC in tracking the DOA, as the source signal polarization changes. Both methods performance degrades when the polarization distinctions among the two source signal decrease. This is evident in the estimation in the middle region of the two figures. However, the performance of the

Fig. 11. MUSIC spectra in time-varying polarization scenario: (a) Polarimetric MUSIC spectra based on the entire data; (b) polarimetric MUSIC tracking; and (c) PTF-MUSIC tracking.

PTF-MUSIC is superior to that of the polarimetric MUSIC when the sources have a time-varying polarization.

IX. CONCLUSION

A platform to deal with diversely polarized sources emitting nonstationary signals with clear time-frequency (t-f) signatures has been introduced. This platform, which is termed *Spatial polarimetric time-frequency distributions (SPTFDs)*, utilizes the polarimetric, spatial, and temporal signatures of signals impinging on an array of sensors. Each sensor is of double-feed, dual-polarized antennas. The SPTFD incorporates the time-frequency distributions (TFD) of the received data across the polarization and spatial variables. It allows the discrimination of sources based on their respective direction-of-arrival as well as their polarization and t-f signal characteristics. The use of TFD reveals the source time-varying frequency natures, and as such, permits the consideration of those t-f points of high signal energy concentrations. The eigen-decomposition of SPTFDs constructed from a portion of, or the entire, t-f signatures of all or a subset of the incoming signals is used to define the polarimetric time-frequency MUSIC (PTF-MUSIC) algorithm. This algorithm is shown to outperform other existing MUSIC methods, including conventional MUSIC, time-frequency MUSIC, and polarimetric MUSIC. For coherent signal environments, the ability to collect the data from the horizontal and vertical polarized antenna arrays, separately, provides the flexibility to trade off subarray and polarization averaging for source matrix rank restoration, and as such, can be used to limit the reduction in array aperture necessary for source decorrelations. The paper considered the application of TFDs to sources with a time-varying polarization in the context of array processing. It has been shown that the difference in the instantaneous polarizations of the sources can be uniquely utilized by the proposed approach to maintain polarization diversity, specifically, in the cases when the source polarizations have similar span of polarization angles over the observation period.

REFERENCES

- [1] L. Cohen, "Time-frequency distributions—A review," *Proc. IEEE*, vol. 77, no. 7, pp. 941–981, Jul. 1989.
- [2] S. Qian and D. Chen, *Joint Time-Frequency Analysis—Methods and Applications*. Englewood Cliffs, NJ: Prentice-Hall, 1996.
- [3] A. Belouchrani and M. G. Amin, "Blind source separation based on time-frequency signal representations," *IEEE Trans. Signal Process.*, vol. 46, no. 11, pp. 2888–2897, Nov. 1998.
- [4] Y. Zhang, W. Mu, and M. G. Amin, "Subspace analysis of spatial time-frequency distribution matrices," *IEEE Trans. Signal Process.*, vol. 49, no. 4, pp. 747–759, Apr. 2001.
- [5] R. O. Schmidt, "Multiple emitter location and signal parameter estimation," *IEEE Trans. Antennas Propag.*, vol. 34, no. 3, pp. 276–280, Mar. 1986.
- [6] R. Roy and T. Kailath, "ESPRIT—estimation of signal parameters via rotational invariance techniques," *IEEE Trans. Acoust., Speech, Signal Process.*, vol. 37, no. 7, pp. 984–995, Jul. 1989.
- [7] A. Belouchrani and M. G. Amin, "Time-frequency MUSIC," *IEEE Signal Process. Lett.*, vol. 6, no. 5, pp. 109–110, May 1999.
- [8] Y. Zhang, W. Mu, and M. G. Amin, "Time-frequency maximum likelihood methods for direction finding," *J. Franklin Inst.*, vol. 337, no. 4, pp. 483–497, Jul. 2000.
- [9] M. G. Amin and Y. Zhang, "Direction finding based on spatial time-frequency distribution matrices," *Digit. Signal Process.*, vol. 10, no. 4, pp. 325–339, Oct. 2000.
- [10] W. C. Y. Lee and Y. S. Yeh, "Polarization diversity for mobile radio," *IEEE Trans. Commun.*, vol. COM-20, no. 5, pp. 912–923, May 1972.
- [11] D. Giuli, "Polarization diversity in radars," *Proc. IEEE*, vol. 74, no. 2, pp. 245–269, Feb. 1986.
- [12] A. I. Kozlov, L. P. Ligthart, and A. I. Logvin, *Mathematical and Physical Modeling of Microwave Scattering and Polarimetric Remote Sensing*. London, U.K.: Kluwer Academic, 2001.
- [13] D. J. McLaughlin, Y. Wu, W. G. Stevens, X. Zhang, M. J. Sowa, and B. Weijers, "Fully polarimetric bistatic radar scattering behavior of forested hills," *IEEE Trans. Antennas Propag.*, vol. 50, no. 2, pp. 101–110, Feb. 2002.
- [14] F. Sadjadi, "Improved target classification using optimum polarimetric SAR signatures," *IEEE Trans. Aerosp. Electron. Syst.*, vol. 38, no. 1, pp. 38–49, Jan. 2002.
- [15] A. L. Pazmany, R. E. McIntosh, R. D. Kelly, and G. Vali, "An airborne 95 GHz dual-polarized radar for cloud studies," *IEEE Trans. Geosci. Remote Sens. Lett.*, vol. 32, no. 4, pp. 731–739, Jul. 1994.
- [16] S. H. Yueh, W. J. Wilson, and S. Dinardo, "Polarimetric radar remote sensing of ocean surface wind," *IEEE Trans. Geosci. Remote Sens.*, vol. 40, no. 4, pp. 793–800, Apr. 2002.
- [17] G. A. Ioannididis and D. E. Hammers, "Optimum antenna polarizations for target discrimination in clutter," *IEEE Trans. Antennas Propag.*, vol. AP-27, no. 3, pp. 357–363, 1979.
- [18] D. A. Garren, A. C. Odom, M. K. Osborn, J. S. Goldstein, S. U. Pillai, and J. R. Guerci, "Full-polarization matched-illumination for target detection and identification," *IEEE Trans. Aerosp. Electron. Syst.*, vol. 38, no. 3, pp. 824–837, Jul. 2002.
- [19] E. R. Ferrara and T. M. Parks, "Direction finding with an array of antennas having diverse polarizations," *IEEE Trans. Antennas Propag.*, vol. 31, no. 2, pp. 231–236, Mar. 1983.
- [20] J. Li and R. J. Compton, "Angle and polarization estimation using ESPRIT with a polarization sensitive array," *IEEE Trans. Antennas Propag.*, vol. 39, no. 9, pp. 1376–1383, Sep. 1991.
- [21] D. Rahamim, R. Shavit, and J. Tabrikian, "Coherent source localization using vector sensor arrays," in *IEEE Int. Conf. Acoustics, Speech, Signal Processing (ICASSP)*, Hong Kong, May 2003.
- [22] Q. Cheng and Y. Hua, "Performance analysis of the MUSIC and PENCIL-MUSIC algorithms for diversely polarized array," *IEEE Trans. Signal Process.*, vol. 42, no. 11, pp. 3150–3165, Nov. 1994.
- [23] K. T. Wong and M. D. Zoltowski, "Self-initiating MUSIC direction finding and polarization estimation in spatio-polarizational beamspace," *IEEE Trans. Antennas Propag.*, vol. 48, no. 9, pp. 1235–1245, Sep. 2000.
- [24] K. T. Wong, L. Li, and M. D. Zoltowski, "Root-MUSIC-based direction-finding and polarization estimation using diversely polarized possibly collocated antennas," *IEEE Antennas Wireless Propag. Lett.*, vol. 3, no. 8, pp. 129–132, 2004.
- [25] B. A. Obeidat, Y. Zhang, and M. G. Amin, "Polarimetric time-frequency ESPRIT," in *Proc. Annu. Asilomar Conf. Signals, Systems, Computers*, Pacific Grove, CA, Nov. 2003, pp. 1178–1182.
- [26] A. B. Gershman and M. G. Amin, "Wideband direction-of-arrival estimation of multiple chirp signals using spatial time-frequency distributions," *IEEE Signal Process. Lett.*, vol. 7, no. 6, pp. 152–155, Jun. 2000.
- [27] N. Ma and J. T. Goh, "DOA estimation for broad-band chirp signals," in *Proc. IEEE Int. Conf. Acoustics, Speech, Signal Processing (ICASSP)*, Montreal, QC, Canada, May 2004, pp. II-261–II-264.
- [28] T. Shan, M. Wax, and T. Kailath, "On spatial smoothing for direction-of-arrival estimation of coherent signals," *IEEE Trans. Acoust., Speech, Signal Process.*, vol. ASSP-33, no. 4, pp. 806–811, Aug. 1985.
- [29] H. Yamada, K. Onishi, and Y. Yamaguchi, "Polarimetric superresolution technique for 2-D radar target imaging," in *SPIE Proc.*, vol. 3120, 1997, pp. 317–326.
- [30] A. Belouchrani, M. G. Amin, and K. Abed-Meraim, "Direction finding in correlated noise fields based on joint block-diagonalization of spatio-temporal correlation matrices," *IEEE Signal Process. Lett.*, vol. 4, no. 9, pp. 266–268, Sep. 1997.
- [31] P. Stoica and A. Nehorai, "MUSIC, maximum likelihood and Cramer–Rao bound," in *IEEE Trans. Acoust., Speech, Signal Process.*, vol. 37, May 1989, pp. 720–741.
- [32] Y. Zhang and M. G. Amin, "Joint Doppler and polarization characterization of moving targets," in *IEEE AP-S Int. Symp. USNC/URSI National Radio Science Meeting*, Monterey, CA, Jun. 2004, pp. 3083–3086.
- [33] M. G. Amin and Y. Zhang, "Bilinear signal synthesis using polarization diversity," *IEEE Signal Process. Lett.*, vol. 11, no. 3, pp. 338–340, Mar. 2004.
- [34] B. A. Obeidat, "Polarimetric array processing for nonstationary signals," M.Sc. thesis, ECE Dept., Villanova Univ., Villanova, PA, 2004.
- [35] W. Mu, M. G. Amin, and Y. Zhang, "Bilinear signal synthesis in array processing," *IEEE Trans. Signal Process.*, vol. 51, no. 1, pp. 90–100, Jan. 2003.



Yimin Zhang (SM'01) received the M.S. and Ph.D. degrees from the University of Tsukuba, Tsukuba, Japan, in 1985 and 1988, respectively.

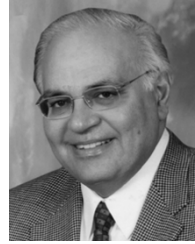
In 1988, he joined the faculty of the Department of Radio Engineering, Southeast University, Nanjing, China. From 1995 to 1997, he served as a Technical Manager at the Communication Laboratory Japan, Kawasaki, Japan, and was a Visiting Researcher at ATR Adaptive Communications Research Laboratories, Kyoto, Japan, from 1997 to 1998. Since 1998, he has been with the Villanova University,

Villanova, PA, where he is currently a Research Associate Professor with the Center for Advanced Communications. His research interests are in the areas of array signal processing, space-time adaptive processing, multiuser detection, MIMO systems, cooperative networks, blind signal processing, digital mobile communications, and time-frequency analysis.



Baha Adnan Obeidat (S'02) was born in Hebron, the West Bank, in 1981. He received the B.S. degree in electrical engineering from Temple University, Philadelphia, PA, in 2002 and the M.S. degree in electrical engineering from Villanova University, Villanova, PA, in 2004.

His research interests include statistical and array signal processing and time-frequency analysis.



Moeness G. Amin (F'00) received the Ph.D. degree from the University of Colorado, Boulder, in 1984.

Since 1985, he has been on the Faculty of Villanova University, Villanova, PA, where is now a Professor in the Department of Electrical and Computer Engineering and the Director of the Center for Advanced Communications. He has over 300 publications in the areas of wireless communications, time-frequency analysis, smart antennas, interference cancellation in broadband communication platforms, direction finding, over-the-horizon radar, radar imaging, and channel equalizations.

Dr. Amin was a Member of the IEEE Signal Processing Society Technical Committee on Signal Processing for Communications from 1998 to 2002 and was a Member of the IEEE Signal Processing Society Technical Committee on Statistical Signal and Array Processing from 1995 to 1997. He was the Technical Chair of the 2nd IEEE International Symposium on Signal Processing and Information Technology, Morocco, 2002; the General and Organization Chair of the IEEE Workshop on Statistical Signal and Array Processing, Pennsylvania, 2000; and the General and Organization Chair of the IEEE International Symposium on Time-Frequency and Time-Scale Analysis, Pennsylvania, 1994. He is the recipient of the IEEE Third Millennium Medal; Distinguished Lecturer of the IEEE Signal Processing Society for 2003; Member of the Franklin Institute Committee of Science and the Arts; recipient of the 1997 Villanova University Outstanding Faculty Research Award; and recipient of the 1997 IEEE Philadelphia Section Service Award. From 1996 to 1998, he was an Associate Editor of the IEEE TRANSACTIONS ON SIGNAL PROCESSING.